A Quadrature Downconversion Autocorrelation Receiver Architecture for UWB

Simon Lee, Sumit Bagga, Wouter A. Serdijn

Electronics Research Laboratory, Faculty of Electrical Engineering, Mathematics and Computer Science (EEMCS)
Delft University of Technology, Delft, the Netherlands
e-mail:{w.k.lee; s.bagga; w.a.serdijn}@ewi.tudelft.nl

ABSTRACT

In this paper, a new UWB receiver architecture is proposed. Unlike a rake receiver, it does not suffer from the timing and template matching problems, and it circumvents processing at high frequencies, thereby reducing the on-chip circuit complexity and power consumption and offering simple but effective narrowband interference rejection. Simulations show that with current IC technology, the receiver only shows a slight, acceptable performance loss with respect to the ideal case.

1. INTRODUCTION

Ultra-wideband (UWB) technology has gained much interest during the last few years as a potential candidate for future wireless short-range data communication. Recently, the FCC has allocated the spectrum from 3.1 GHz to 10.6 GHz for UWB applications. Due to its large bandwidth UWB has the promise of high data rates [1].

A particular type of UWB communication is impulse radio [2], where very short transient pulses are transmitted rather than a modulated carrier. Consequently, the spectrum is spread over several gigaherz, complying with the definition of UWB.

Currently, the rake receiver is considered to be a very promising candidate for UWB reception, due to its capability of collecting multipath components [3]. Rake receivers perform detection by correlating the incoming pulse with a locally generated template pulse, which is tacitly assumed to be perfectly synchronized to the incoming pulse. However, perfect synchronization can never be accomplished.

Another issue is the matching of the template with the received pulse. Since the antennas and the channel are frequency selective, thereby causing dispersion and ringing, the transmitted pulse becomes severely distorted and hence it is unlikely that the received pulse corresponds to the template pulse.

Not much is published on the actual implementation of rake receivers. Moreover, often a lot of rake fingers are required to accommodate the wireless channel, rendering it not favourable from an implementation point of view. Indeed low complexity rake receivers are being investigated [4].

The transmitted reference scheme proposed by Hoctor and Tomlinson [5] does not suffer from the above problems and requires fewer RF building blocks compared to the multiple finger rake receiver. The core part of the transmitted reference scheme receiver, alternatively known as "autocorrelation receiver", is shown in Fig. 1.

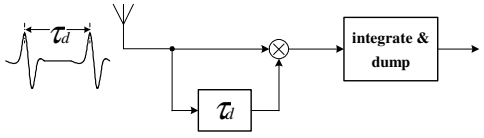

Figure 1: An autocorrelation receiver with a typical waveform

In the transmitted reference scheme, two pulses per symbol are sent with a certain chosen delay τ_d between them. The first pulse acts as the reference and the second pulse is the modulated one. The receiver delays the first pulse by the delay τ_d, multiplies it with the second pulse and integrates the result over one delay length, which in fact correlates the two pulses. When using polar NRZ modulation, for a logical zero, a pulse $g(t)$ is transmitted, subsequently followed by a polarity reversed pulse $-g(t)$. To send a logical one, two pulses with the same polarity are sent sequentially. Instead of transmitting two pulses for each symbol, it is also possible to use the previous pulse as the reference, resulting in differential coding. The absolute value of the output after integration is in fact the energy of the pulse while the polarity of the output contains the data. If the output is negative, this corresponds to a logical zero, while a positive output corresponds to a logical one. Thus, the information is in the relative polarity of the two pulses and the delay between them acts as a synchronization mechanism. As long as the two consecutive pulses have corresponding waveforms except for their polarity, the autocorrelation receiver can detect them properly.

Yet, directly processing at UWB frequencies, due to the inherent influence of on-chip parasitic reactances at these frequencies, requires relatively large currents, or the use of expensive high speed technologies (SiGe, GaAs) that are not compatible with mainstream CMOS IC technology for mass market use.

Another important issue is narrowband interference. Since UWB systems transmit at a low spectral density, it is very likely that existing narrowband systems with relatively high power will jam the UWB system, even though UWB systems are claimed to have high processing gain [6]. Most solutions in literature propose MMSE combining of the rake fingers [6, 7] to combat narrowband interference. Both the normal rake receiver and the autocorrelation receiver suffer from narrowband interference. It is expected that the IEEE802.11a

and HiperLAN wireless LAN systems around 5 GHz, which is in the middle of the UWB spectrum, generate most of the interference [8, 9]. Additionally, although the UWB antenna may do some out-of-band filtering, due to their relatively high power levels, it is even likely that signals originating from wireless LAN systems operating around 2.4 GHz and even GSM can penetrate into the system, causing jamming of the UWB system.

This paper suggests a new receiver architecture based on the transmitted reference scheme from Hoctor and Tomlinson [5] for its mentioned advantages with respect to the rake receiver. It deals with interference rejection by filtering and avoids high frequency on-chip processing by using frequency conversion. Section 2 gives a detailed analysis of the system. Section 3 presents the simulation results, followed by the conclusions in Section 4. Figure 2 shows the proposed receiver architecture.

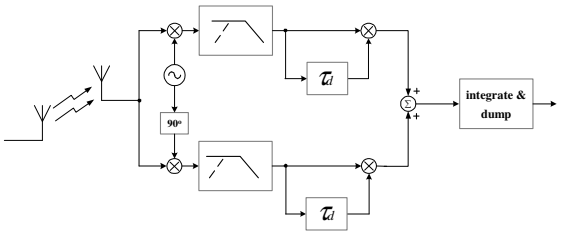

Figure 2: The quadrature downconversion autocorrelation receiver

2. SYSTEM ANALYSIS

The proposed architecture employs frequency conversion. Its oscillator frequency is chosen such that the spectrum wraps around DC. In conventional narrowband systems downconversion is applied to have the processing at lower frequencies, reducing on-chip circuit complexity and power consumption. Normally, downconversion systems suffer from limited image rejection. In the case of UWB there is not such a thing as an image since the spectrum is already a couple of gigaherz wide and the "image" is part of the desired UWB spectrum. Hence, if the oscillator frequency is chosen such that the UWB spectrum is down-converted and even wraps around the origin, the signal bandwidth is lowered and reduced. Moreover, interferers below 3.1 GHz can be up-converted, making it possible to remove them with a low-pass filter.

In traditional narrowband systems frequency wrapping is not possible, as the resulting bandwidth must equal the original bandwidth. Here, since we are dealing with short-transient pulses, frequency wrapping is allowed. Of course, after downconversion the waveform is changed, but as long as the two received consecutive pulses are distorted equally and we are able to discriminate individual pulses, which is the case, the autocorrelation receiver is able to detect the signal correctly.

We will now make a proper choice for the frequency of the local oscillator (LO). If the LO frequency is set to the center frequency of the pulse, which for simplicity is chosen to be in the middle of the band allocated by the FCC for UWB (6.85 GHz), the system acts like a zero IF system and the bandwidth is halved, i.e., the band from 3.1 GHz to 10.6 GHz is transformed into a baseband signal from DC to 3.75 GHz. However, the wireless LAN originally residing at around 5.5 GHz is shifted to 1.35 GHz, so it is still in band. Yet, at these frequencies it is much easier to filter out the interferer on chip than at its original frequency. Another option is to set the oscillator frequency to this wireless LAN frequency such that this interferer is shifted to around zero, making it possible to remove it with a simple high-pass or band-pass filter. A possible disadvantage is that the down-converted bandwidth of the UWB signal extends up to approximately 5.1 GHz and the converted 2.4 GHz interferer falls in band.

A third option is to set the LO to 5.5 GHz and filter out below (5.5 – 5.15 =) 0.35 GHz and above (5.5 – 2.4 =) 3.1 GHz. By this we remove the interferers completely with a simple band-pass filter, albeit at the expense of the loss of part of the incoming frequency band, from (5.5 + (5.5 – 2.4)) = 8.6 GHz tot 10.6 GHz and from 5.15 to 5.85 GHz, which is a bandwidth of 2.7 GHz, being only 36%, or equivalently 1.9 dB. The UWB spectrum before and after downconversion is illustrated in Fig. 3. The local oscillator is also shown.

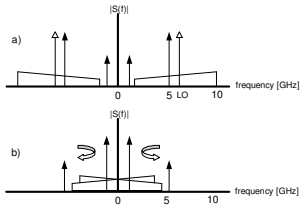

Figure 3: The UWB spectrum with narrowband interferers at 2.4 GHz and 5 GHz a) before downconversion and b) after downconversion

2.1 Time Domain Analysis

Because UWB systems rely on timing information, we will use a time domain analysis throughout the remainder of this paper. Any physical band-pass waveform can be represented by:

$$A(t)\cos(\omega_c t + \varphi(t)) \tag{1}$$

where $A(t)$ is the amplitude envelope, ω_c is the carrier frequency and $\varphi(t)$ is the phase modulation. This description is commonly used for carrier-based signals but can also be applied to pulse-based signals as long as they have a band-pass spectrum. Although (1) is applicable to the generally used first and second derivative of the Gaussian pulse, for simplicity of the analysis to come, the pulse used, $g(t)$, is chosen to be the real part of a Morlet, defined to be:

$$g(t) = e^{-t^2/2\sigma^2}\cos(\omega_c t) \tag{2}$$

where σ determines the pulse width and ω_c is the center frequency of the spectrum. In Fig. 4, a Morlet is shown with a pulse width of 1 ns and a center frequency of 4.5 GHz, along with its spectrum.

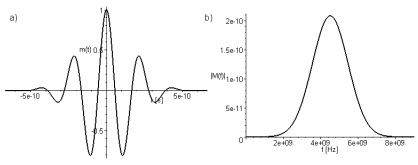

Figure 4: A typical Morlet a) waveform with a pulse width of 1 ns and center frequency of 4.5 GHz and b) its frequency spectrum

Equating (1) to (2) shows that $A(t)$ is just the Gaussian envelope, ω_c is the center frequency and $\varphi(t) = 0$.

Now consider the situation where two pulses of equal sign are transmitted. For the moment, assume that we only have the upper path of the circuit shown in Fig. 2. This path is denoted here as the in-phase path. After mixing with a cosine of angular frequency ω_{osc} and a normalized amplitude of one and using (1), we obtain for the first pulse:

$$g(t)\cos(\omega_{osc}t) = A(t)\cos(\omega_c t)\cos(\omega_{osc}t) \quad (3)$$

Assuming an ideal low-pass filter and using $\cos(a)\cos(b) = \frac{1}{2}[\cos(a+b) + \cos(a-b)]$, the signal after filtering becomes:

$$\frac{A(t)}{2}\cos((\omega_c - \omega_{osc})t) \quad (4)$$

After delaying this first pulse in the delayed path:

$$\frac{A(t-\tau_d)}{2}\cos((\omega_c - \omega_{osc})(t-\tau_d)) \quad (5)$$

To ease the analysis, a change of variable is made by letting $t' = t - \tau_d$:

$$\frac{A(t')}{2}\cos((\omega_c - \omega_{osc})t') \quad (6)$$

This is the signal in the delayed path before the multiplier.

For the second pulse the same analysis holds but the input is now a pulse delayed by τ_d in the transmitter:

$$g(t-\tau_d)\cos(\omega_{osc}t) = A(t-\tau_d)\cos(\omega_c(t-\tau_d))\cos(\omega_{osc}t) \quad (7)$$

The signal after the low-pass filter equals:

$$\frac{A(t-\tau_d)}{2}\cos(\omega_c(t-\tau_d) - \omega_{osc}t) \quad (8)$$

Again, after a change of variable $t' = t - \tau_d$:

$$\frac{A(t')}{2}\cos((\omega_c - \omega_{osc})t' - \omega_{osc}\tau_d) \quad (9)$$

The signal before integration is obtained by multiplication of (6) and (9), resulting in:

$$\frac{A^2(t')}{4}\cos((\omega_c - \omega_{osc})t')\cos((\omega_c - \omega_{osc})t' - \omega_{osc}\tau_d) \quad (10)$$

This can be rewritten as:

$$\frac{1}{2}\frac{A^2(t')}{4}\left[\cos(2(\omega_c - \omega_{osc})t') + \cos(\omega_{osc}\tau_d)\right] \quad (11)$$

For a transmitted logical zero, the output is just (11) with a minus sign in front. From (11) it can be seen that only if $\omega_{osc}\tau_d = 2\pi n$, where $n \in \aleph$, the output is fully positive or fully negative, depending on the transmitted symbol. The output after the integrate-and-dump filter is thereby in absolute sense maximized. This means that if $\omega_{osc}\tau_d \notin 2\pi n$, the performance will degrade. E.g., $\omega_{osc}\tau_d = \frac{1}{2}\pi$ even causes the output to be zero, irrespective of the transmitted data and detection is not possible. Together with the above frequency conversion analysis, this puts a second constraint on the choice of the oscillator frequency.

2.2 The Quadrature Downconversion Autocorrelation Receiver Architecture

The previous analysis assumed perfect synchronization between the oscillator and the "pulse carrier". In reality this is not the case. Unless the oscillator is being locked onto the incoming signal there is always a relative phase between the oscillator and the "pulse carrier". Denoting this relative phase by φ_0 this means that in (3) and (7) $\omega_{osc}t$ has to be replaced by $\omega_{osc}t + \varphi_0$. Following the same analysis as before, it can be found that the signal before integration now equals:

$$\frac{1}{2}\frac{A^2(t')}{4}\left[\cos(2(\omega_c - \omega_{osc})t' - \varphi_0) + \cos(\omega_{osc}\tau_d)\right] \quad (12)$$

If $\omega_{osc} = \omega_c$, this means that after integration the result depends on φ_0. The output can even be zero whereas a positive value was expected. This is a well-known phenomenon in coherent detection. In coherent detection, the oscillator can be locked to the carrier but since in this situation there is a suppressed very weak carrier that is only present when the pulse is present and there is also narrowband interference, this is not possible. A possible solution is to add a similar path but now mixed with a sine instead of a cosine and add the outputs after autocorrelation, resulting in the architecture shown in Fig. 2. This lower path is called the quadrature path from now on. For this quadrature path, it holds that the signal after multiplication and before integration becomes:

$$\frac{1}{2}\frac{A^2(t')}{4}\left[-\cos(2(\omega_c - \omega_{osc})t' - \varphi_0) + \cos(\omega_{osc}\tau_d)\right] \quad (13)$$

Now adding the two quadrature autocorrelation signals given by (12) and (13) results in the signal before integration:

$$\frac{A^2(t')}{4}\cos(\omega_{osc}\tau_d) \quad (14)$$

(14) shows that the output does not depend on φ_0 anymore. The influence of the relation between ω_{osc} and τ_d is obvious. For a transmitted logical zero it can be found that the output is:

$$-\frac{A^2(t')}{4}\cos(\omega_{osc}\tau_d) \quad (15)$$

2.3 Analysis of the Quadrature Downconversion Autocorrelation Receiver Subject to Mismatch

The previous analysis assumed ideal phase and amplitude relations between the two paths. When implemented, these relations will never be exact due to component mismatch. Also, the delays and the oscillator period will show some variation. It is important to analyze the performance of the architecture when these errors are taken into account.

The following errors are considered:

- The mismatch between the delay in the transmitter and in the receiver. This can be taken into account by introducing τ_{tx} and τ_{rx}, where τ_{tx} denotes the delay in the transmitter and τ_{rx} indicates the delay in the receiver.
- The phase mismatch between the cosine and sine, originating from an imperfect quadrature relation. This phase error is denoted by φ_e.
- The amplitude mismatch in the two paths, which can be modelled by assigning the oscillators in the in-phase and quadrature path a different amplitude A_I and A_Q respectively.
- The error in the ratio of the delay and the oscillator period, *n*.

Hence, all these errors can be taken into account by replacing $\cos(\omega_{osc}t + \varphi_0)$ by $A_I\cos(\omega_{osc}t + \varphi_0)$ and $\sin(\omega_{osc}t + \varphi_0)$ by $A_Q\sin(\omega_{osc}t + \varphi_0 \pm \varphi_e)$ in the previous analysis, where φ_e is defined to be positive. In the previous derivations the delay in the transmitter was assumed to be the same as in the receiver, both being equal to τ_d. With the introduction of mismatch between these delays, if the delaying action is due to the transmitter delay, τ_d has to be replaced by τ_{tx}, while τ_d has to be replaced by τ_{rx} if the delaying is due to the receiver. With these substitutions, for the in-phase path, the signal after multiplication and before addition becomes:

$$\frac{1}{2}\frac{A_I^2 A(t')A(t'+\Delta\tau)}{4}\begin{bmatrix}\cos(2(\omega_c-\omega_{osc})t'-\varphi_0)+\\ \cos(\omega_c\Delta\tau-\omega_{osc}\tau_d)\end{bmatrix} \quad (16)$$

where $\Delta\tau = \tau_{rx} - \tau_{tx}$. For the quadrature path, the corresponding signal becomes:

$$\frac{1}{2}\frac{A_Q^2 A(t')A(t'+\Delta\tau)}{4}\begin{bmatrix}-\cos(2(\omega_c-\omega_{osc})t'-\varphi_0\pm\varphi_e)+\\ \cos(\omega_c\Delta\tau-\omega_{osc}\tau_d)\end{bmatrix} \quad (17)$$

Adding both paths results in:

$$\begin{aligned}&(A_I^2+A_Q^2)\frac{1}{2}\frac{A(t')A(t'+\Delta\tau)}{4}\cos(\omega_c\Delta\tau-\omega_{osc}\tau_{rx})+\\ &\frac{1}{2}\frac{A(t')A(t'+\Delta\tau)}{4}\begin{bmatrix}-A_Q^2\cos(2(\omega_c-\omega_{osc})t'-\varphi_0\pm\varphi_e)+\\ A_I^2\cos(2(\omega_c-\omega_{osc})t-\varphi_0)\end{bmatrix}\end{aligned} \quad (18)$$

Consider the first part of (18). Suppose $A_Q = (1 \pm \alpha)A_I$ to denote the amplitude mismatch, where $0 < \alpha < 1$. Then the first part of (18) results in:

$$\begin{aligned}&(A_I^2+(1\pm\alpha)^2A_I^2)\frac{1}{2}\frac{A(t')A(t'+\Delta\tau)}{4}\cos(\omega_c\Delta\tau-\omega_{osc}\tau_{rx})=\\ &(2+\alpha^2\pm2\alpha)A_I^2\frac{1}{2}\frac{A(t')A(t'+\Delta\tau)}{4}\cos(\omega_c(\tau_{rx}-\tau_{tx})-\omega_{osc}\tau_{rx})=\\ &(1+\frac{\alpha^2}{2}\pm\alpha)A_I^2\frac{A(t')A(t'+\Delta\tau)}{4}\cos\begin{bmatrix}(\omega_c-\omega_{osc})\tau_{rx}-\\ \omega_c(1\pm\beta)\tau_{rx}\end{bmatrix}=\\ &(1+\frac{\alpha^2}{2}\pm\alpha)A_I^2\frac{A(t')A(t'+\Delta\tau)}{4}\cos(\omega_{osc}\tau_{rx}\pm\beta\omega_c\tau_{rx})\end{aligned} \quad (19)$$

where β denotes the relative mismatch between the delay in the transmitter and receiver. It holds: $0 < \beta < 1$. For the argument in the cosine in (19), it can be written:

$$\omega_{osc}\tau_{rx}\pm\beta\omega_c\tau_{rx} = 2\pi(\frac{\tau_{rx}}{T_{osc}}\pm\beta\frac{\tau_{rx}}{T_c}) \quad (20)$$

Where T_{osc} is the oscillator period and T_c is the inverse of the pulse center frequency.

Now considering the second part of (18):

$$\begin{aligned}&\frac{1}{2}\frac{A(t')A(t'+\Delta\tau)}{4}\begin{bmatrix}-A_Q^2\cos(2(\omega_c-\omega_{osc})t'-\varphi_0\pm\varphi_e)+\\ A_I^2\cos(2(\omega_c-\omega_{osc})t-\varphi_0)\end{bmatrix}=\\ &\frac{1}{2}\frac{A(t')A(t'+\Delta\tau)}{4}\begin{bmatrix}A_I^2\cos(2(\omega_c-\omega_{osc})t-\varphi_0)-\\ (1\pm\alpha)^2A_I^2\cos(2(\omega_c-\omega_{osc})t'-\varphi_0\pm\varphi_e)\end{bmatrix}=\\ &\frac{1}{2}\frac{A(t')A(t'+\Delta\tau)}{4}\begin{Bmatrix}A_I^2\begin{bmatrix}\cos(2(\omega_c-\omega_{osc})t-\varphi_0)-\\ \cos(2(\omega_c-\omega_{osc})t'-\varphi_0\pm\varphi_e)\end{bmatrix}-\\ (\alpha^2\pm2\alpha)A_I^2\cos(2(\omega_c-\omega_{osc})t'-\varphi_0\pm\varphi_e)\end{Bmatrix}\end{aligned} \quad (21)$$

Using $\cos(a) - \cos(b) = -2\sin(\frac{1}{2}(a+b))\sin(\frac{1}{2}(a-b))$, we get:

$$\begin{aligned}&\frac{1}{2}\frac{A(t')A(t'+\Delta\tau)}{4}\\ &\begin{Bmatrix}A_I^2\begin{bmatrix}-2\sin(2(\omega_c-\omega_{osc})t-\varphi_0\pm\frac{\varphi_e}{2})\sin(\pm\frac{\varphi_e}{2})\end{bmatrix}-\\ (\alpha^2\pm2\alpha)A_I^2\cos(2(\omega_c-\omega_{osc})t'-\varphi_0\pm\varphi_e)\end{Bmatrix}=\\ &-\frac{A(t')A(t'+\Delta\tau)}{4}A_I^2\begin{bmatrix}\sin(2(\omega_c-\omega_{osc})t-\varphi_0\pm\frac{\varphi_e}{2})\sin(\pm\frac{\varphi_e}{2})+\\ (\frac{\alpha^2}{2}\pm\alpha)\cos(2(\omega_c-\omega_{osc})t'-\varphi_0\pm\varphi_e)\end{bmatrix}\end{aligned} \quad (22)$$

Since for any t:

$$\left|\begin{bmatrix}\sin(2(\omega_c-\omega_{osc})t-\varphi_0-\frac{\varphi_e}{2})\sin(\frac{\varphi_e}{2})+\\ (\frac{\alpha^2}{2}\pm\alpha)\cos(2(\omega_c-\omega_{osc})t'-\varphi_0-\varphi_e)\end{bmatrix}\right| \le \sin(\frac{\varphi_e}{2})+(\frac{\alpha^2}{2}+\alpha) \quad (23)$$

it holds that the absolute value of the second part is always smaller than

$$\pm\frac{A(t')A(t'+\Delta\tau)}{4}A_I^2\left[\sin(\frac{\varphi_e}{2})+(\frac{\alpha^2}{2}\pm\alpha)\right] \quad (24)$$

Now adding part 1 and part 2 yields the output before integration to be larger or equal to

$$\pm A_I^2\frac{A(t')A(t'+\Delta\tau)}{4}\begin{bmatrix}(1+\frac{\alpha^2}{2}-\alpha)\cos(\omega_{osc}\tau_{rx}\pm\beta\omega_c\tau_{rx})-\\ \sin(\frac{\varphi_e}{2})-(\frac{\alpha^2}{2}+\alpha)\end{bmatrix} \quad (25)$$

Note that this is a worst-case situation given a certain α, β and φ_e. In the ideal case (α, β, $\varphi_e = 0$) the result would be (if the nominal oscillator amplitude would be A_I):

$$\pm A_I^2\frac{A^2(t')}{4} \quad (26)$$

Compared to (26) the result of (25) shows some degradation due to the phase mismatch, the amplitude mismatch and the mismatch between the delays in the transmitter and the receiver. In case of a Gaussian envelope, the degradation due to the term $A(t')A(t' + \Delta\tau)$ is relatively small.

3. RESULTS

To verify the functional behaviour of the proposed receiver, the system was simulated in Matlab/Simulink, assuming interference and multipath to be absent. These assumptions are justified as interference can be dealt with by means of a band-pass filter. Since the multipath components are resolvable, they will add up.

A Morlet was used with a center frequency of 4.5 GHz, an effective pulse width of 1ns and a peak amplitude of one. The oscillator frequency was set to 4.6 GHz. A pulse repetition time of 10 ns was used, which corresponds to a bit rate of 100 Mb/s. The input consisted of five pulses with random polarity, representing a sequence of five differentially coded random data bits. Also to verify the concept, a sub-optimal second-order low-pass Butterworth characteristic with a cut-off frequency of 4.5 GHz was chosen for both filters.

First, the ideal situation was simulated. The initial phase of the oscillator was set to zero; the delay in the receiver matched the delay between the pulses in the transmitter (equal to the pulse repetition time) and the oscillator period was a perfect integer of this delay; no amplitude mismatch was present in the two paths and the oscillator signals had a perfect quadrature relation; the oscillator amplitude in both paths was set to one. The absolute value of the integrator output in this ideal case serves as the reference value, as from the analysis in Section 2.3 it followed that any mismatch appearing in the system will degrade the output value. All subsequent results will be normalized to this value to show the performance loss. Fig. 5 shows the pulses in both paths after downconversion and filtering and the integrator output in this ideal case.

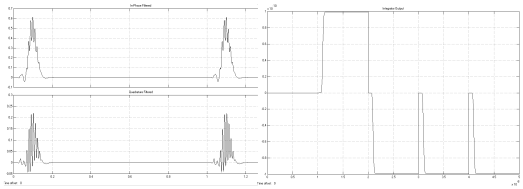

Figure 5: Two consecutive pulses in both paths after downconversion and filtering (left) and integrator output for the data sequence 1000 (right) in the ideal case

Secondly, the initial phase was varied from 0° to 360° in steps of 10°. In line with the analysis of Section 2.2 the output shows no degradation with respect to the ideal value.

Thirdly, the influence of the amplitude mismatch was simulated by adding a gain block after the oscillator in the quadrature path, its gain being equal to (1-α), α ranging from 0 to 0.05 in steps of 0.005. The normalized output value as a function of α is shown in Fig. 6.

The effect of the phase error between the two paths on the output was evaluated by adding an additional phase shift of 0 to 5 degrees in steps of a half degree to the oscillator in the quadrature path (after removing the amplitude mismatch). Fig. 6 shows the normalized output as a function of the phase error.

The mismatch between the delay in the transmitter and the receiver was simulated by setting the pulse repetition time in the generator to (1 + β) of its nominal value (10 ns) and varying β from 0 to 0.005 in steps of 0.001. The normalized output as a function of β is shown in Fig. 7.

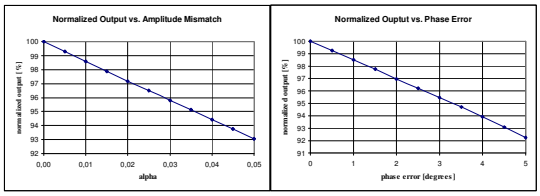

Figure 6: Normalized output as a function of the amplitude mismatch (left) and the phase error (right)

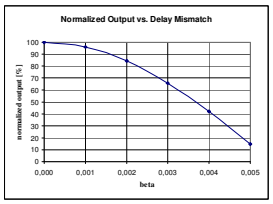

Figure 7: Normalized output as a function of the relative delay mismatch

With current IC technology, α, β and φ_e can be readily made smaller than 2%, 5% and 2°, respectively. From Fig. 6 and Fig. 7 it can be seen that the mismatch between the delay in the transmitter and in the receiver plays a dominant role in the performance loss. Compared to this delay mismatch, the performance degradation due to the amplitude mismatch and phase error is negligible. Therefore, the design of matching delays should get most attention. Without additional measures, in current IC technology, β is one order in magnitude larger than allowed for acceptable performance loss. To overcome this, one can lock the delays to a highly accurate time reference such as a crystal. The delay mismatch then relies on the mismatch between the crystals, which can be as small as 0.001, yielding an acceptably small performance loss. A worst-case combined error simulation with α = 0.02, φ_e = 2° and β = 0.002 shows that the normalized output is still as high as 80%, equivalent to a loss of only 1.9 dB.

4. CONCLUSION

A new UWB receiver architecture has been introduced. It avoids high frequency processing, allowing for reduction of the on-chip circuit complexity and power consumption and rejects narrowband interference in a simple but effective way. Assuming component matching that can be readily achieved in today's IC technologies, Matlab/Simulink simulations show that the output only shows a performance loss up to 1.9 dB compared to the ideal case. The mismatch between the delay in the transmitter and the receiver is the largest contributor to this degradation.

ACKNOWLEDGEMENTS

This work is part of the AIRLINK project of Delft University of Technology (www.airlink.tudelft.nl) and partially sponsored by the Ministry of Economical Affairs under the Dutch Initiative "Freeband."

5. REFERENCES

[1] J. Foerster, E. Green, S. Somayazulu and D. Leeper, "Ultra-Wideband Technology for Short- or Medium-Range Wireless Communications," *Intel Technology Journal Q2*, 2001

[2] M.Z. Win and R.A. Scholtz, "Impulse Radio: How it works," *IEEE Comm. Letters*, vol. 2, pp. 36-38, Feb. 1998

[3] J.G. Proakis, *Digital Communications*, 3rd ed. McGraw-Hill, 1995

[4] D. Cassioli, M.Z. Win, F. Vatalaro and A.F. Molisch, "Performance of Low-Complexity Rake Reception in a Realistic UWB Channel," *Proceedings of the IEEE International Conference on Communications*, vol. 2, pp. 763-767, May 2002

[5] R.T. Hoctor and H.W. Tomlinson, "Delay-Hopped Transmitted-Reference RF Communications," *Proceedings of the IEEE Conference on Ultra Wideband Systems and Technologies*, pp. 265-270, May 2002

[6] I. Bergel, E. Fishler and H. Messer, "Narrow-band Interference Suppression in Time-Hopping Impulse-Radio Systems," *Proceedings of the IEEE Conference on Ultra Wideband Systems and Technologies*, pp. 303-308, May 2002

[7] Q. Li, and L.A. Ruch, "Hybrid RAKE/Multiuser Receivers for UWB," *Proceedings of the Radio and Wireless Conference*, pp. 203-206, Aug. 2003

[8] M. Hämäläinen, V. Hovinen, R. Tesi, J. Iinatti and M. Latva-aho, "On the UWB System Coexistence with GSM900, UMTS/WCDMA, and GPS," *IEEE Journal on Selected Areas in Communications*, vol. 20, pp. 1712-1721, Dec. 2002

[9] M. Hämäläinen, R. Tesi and J. Iinatti, "On the UWB System Performance Studies in AWGN Channel with Interference in UMTS Band," *Proceedings of the IEEE Conference on Ultra Wideband Systems and Technologies*, pp. 321-326, May 2002